Universitat Politècnica de Catalunya (UPC)
Universitat Autònoma de Barcelona (UAB)
Universitat de Barcelona (UB)
Institut de Ciències Fotòniques (ICFO)

http://www.photonicsbcn.eu

Master in Photonics

MASTER THESIS WORK

Characterization of femtosecond pulses from *xz* BIBO OPO

Enrique Sánchez Bautista

Supervised by Dr. Adolfo Esteban Martín (ICFO) and Prof. Dr. Majid Ebrahim Zadeh (ICFO)

Presented on date 10th of September of 2012

Registered at

ETSETB Escola Tècnica Superior d'Enginyeria de Telecomunicació de Barcelona

Characterization of femtosecond pulses from xz BIBO OPO

Enrique Sánchez Bautista

Optical Parametric Oscillators Group, Institute of Photonic Sciences (ICFO).
Av. Carl Friedrich Gauss, nº3, 08860 Castelldefels, Barcelona, Spain.

E-mail: enrique.sanchez@icfo.es

Abstract. We demonstrate a self-phase-locked divide-by-2 synchronously pumped optical parametric oscillator (SPOPO) based on BiB_3O_6 (BIBO) a crystal with type I interaction in the *xz* plane operating in degenerate regime. The femtosecond SPOPO is pumped by a KLM Ti:sapphire and uses a 1.5 mm long BIBO crystals cut for collinear type I ($e \rightarrow o + o$) PM in the *xz* optical plane at an internal angle $\theta = 11.4^{o}$ ($\phi = 0^{o}$) at normal incidence. The phase-locking operation was confirmed by splitting at the beginning the pump into two experimental lines (divided-by-2) overlapping them at the end of the experimental line setting a Mach-Zehnder interferometer. The SPOPO signal and idler output (1.5 μm and 1.6 μm aprox. respectively) was frequency doubled (SHG) and after was overlapped with the pump. The observation of stationary fringes from the interference established phase coherence. Additionally, we report the generation of a toothed shape in the spectrum of the overlapped signal and idler pulses of the SPOPO across 1.5-1.6 μm and 1.6-1.7 μm respectively in the degeneracy regime which can suggest the fact that an optical comb might have been generated.

Keywords: OPO, Optical frequency combs, optical interferometry, OPG ($e \rightarrow o + o$), SHG ($o + o \rightarrow e$), degenerated OPO.

1. Introduction

1.1. *Motivation of the project*

New and outstanding experiments in the field of frequency metrology are a significant step toward next-generation "atomic clocks" based on optical rather than microwave frequencies expecting to be even more than 100 times more accurate than today's best time-keeping systems [1]. Better clocks based in frequency comb technology will enable to use and improve in many other research fields and technologies, from medical tests in doctor's offices, to synchronization of advanced telecommunications systems and precision navigation systems such as next-generation global positioning systems, to remote detection and range measurements for manufacturing or defense applications. Highly accurate measurements of frequencies are also essential for many other advanced fields of science that require the identification or manipulation of atoms or molecules, such as detection of toxic biochemical agents, studies of ultrafast dynamics and quantum computing.

The motivation of this project that led to the writing of this master thesis project has been to generate a broad, fixed frequency comb by using a self-phase-locked degenerate femtosecond optical parametric oscillator.

2. Introduction (principles of operation)

2.1. Introduction to nonlinear optics: polarization and processes. Second-order nonlinear frequency conversion. Optical parametric oscillators. Phase Matching condition.

When a dielectric material interacts the interaction of an electro-magnetic field, the result is an induced polarization field in the material. Normally, the response of the material is linear, making penetration and propagation of several electro-magnetic waves inside the material without any interaction between waves. However, when the incident electro-magnetic fields are intense enough, an induced polarization can appear due to nonlinear properties. This effect derives from the higher order terms of the electromagnetic field contained in the expression of the polarization vector:

$$P_i = \chi_{ij}^{(1)}\varepsilon_0 E_j + \chi_{ijk}^{(2)}\varepsilon_0 E_j E_k + \chi_{ijkl}^{(3)}\varepsilon_0 E_j E_k E_l + \ ... = P_L + P_{NL} \tag{2.1}$$

where *i*, *j*, *k*, *l* indices are related with the coordinates frame, ε_0 is the permittivity of free space, $\chi_{ij}^{(1)}$ is the linear susceptibility and $\chi_{ijk}^{(2)}$ and $\chi_{ijkl}^{(3)}$ are the tensors of second and third order nonlinear optical susceptibilities. The first term accounts for the linear part of the polarization vector whereas the second, the third and beyond account for the nonlinear contribution to the polarization vector.

In the context of this master thesis, we concentrate on the second-order term which contains second-order nonlinear susceptibility factor $\chi^{(2)}$. These second-order nonlinear effects can be achieved only in a certain group of dielectric crystals with non-centrosymmetric structures. This includes crystals like lithium niobate ($LiNbO_3$), MgO-doped periodically poled lithium niobate (MgO-doped PPLN), potassium titanyl phosphate (KTP, $KTiOPO_4$), potassium dihydrogen phosphate (KDP, KH_2PO_4), lithium triborate (LBO, LiB_3O_5), β-barium borate (BBO, β-BaB_2O_4), bismuth triborate (BIBO, BiB_3O_6), etc.

Different harmonic and parametric processes can be achieved from the second-order nonlinear susceptibility tensor $\chi_{ijk}^{(2)}$. Some of them can be observed in Fig. 1 and they can be divided in two groups as explained in the Fig. 1. In this master thesis, our experiment is focused in OPO in addition to SFG, which plays an important role in one part of the experiment. In all these frequency conversion processes the energy of the photons that take part in the mixing has to be conserved because of the principle of energy conservation.

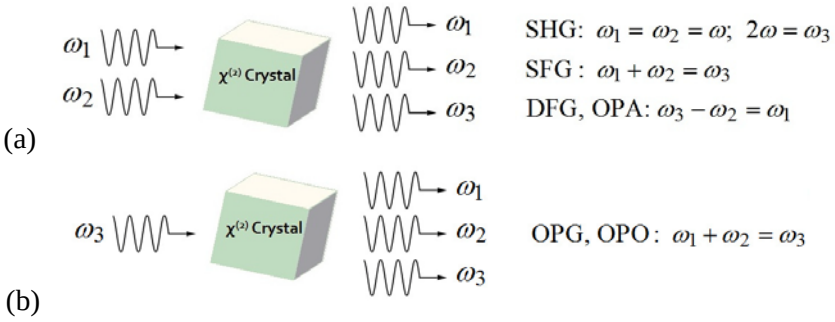

Figure 1. Schematic diagram of the second-order nonlinear processes: (a) shows the processes when two electromagnetic waves impinge on the dielectric material: second-harmonic generation (SHG), sum-frequency generation (SFG), difference-frequency generation (DFG) and optical parametric amplification (OPA); (b) shows the processes when there is only one incident field to the material: optical parametric generation (OPG).

2.2. Introduction to Optical Parametric Oscillators

OPOs basically are devices made of a nonlinear medium in an optical cavity pumped by a laser source that efficiently converts a high energy pump photon into two lower energy photons. The two beams originated in the process are called signal and idler. By convention, they have the shorter and the longer wavelength respectively.

In this nonlinear frequency conversion process, it is strictly necessary that any pair of photons at different frequencies satisfy the energy conservation condition:

$$\omega_p = \omega_s + \omega_i \tag{2.2}$$

where ω_p, ω_s and ω_i correspond to pump, signal and idler frequencies. Regarding the output signal produced by this kind of devices, they can be assumed similar to a laser in terms of properties of the generated light. Thus, the generated light by an OPO is identical to a light generated by laser, since both are coherent, monochromatic and collimated sources. Furthermore, the final output frequencies (ω_s and ω_i) can be tunable by adjusting parameters such as, crystal temperature, incident angle, applied electric field and pump wavelength, which implies a great advantage of the OPOs compared with a common laser device [2].

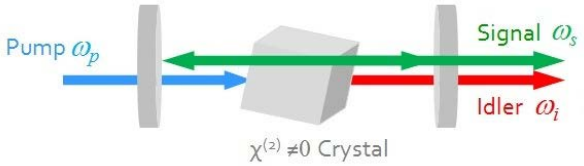

Figure 2. Basic structure of an OPO in which the pump laser, the signal and the idler beams are represented.

The final output frequencies are determined by other constraints like the gain mechanism inside crystal, the losses experienced at the mirrors as well as some properties of the dielectric crystal. Moreover, every photon in the device should accomplish the momentum conservation, or phase-matching condition to get amplified (see more in Section 2.3).

When the pump light is not delivered continuously and it is delivered in the form of ultrashort pulses synchronized with the pulses inside the OPO instead, they receive the name of Synchronously-Pumped Optical Parametric Oscillators (SPOPOs). This option is only suitable for ultrashort pulse generation, because a parametric device is not able to store the pump energy for use at later times [3].

2.3. Introduction to Phase-Matching

When an electromagnetic wave with wavelength λ_n is propagating in an optical medium, the wave-vector corresponding to this medium is

$$k_n = \frac{2\pi}{\lambda_n} \tag{2.3}$$

being n the refractive index of the crystal. In nonlinear materials, the refractive index it is function of the wavelength, $n(\lambda)$. Thus, different waves with different wavelengths do not have the same phase velocities: for an electromagnetic wave with wavelength λ, propagating in an optical medium, $v_p = \frac{\omega}{k_n} = \frac{\omega\lambda}{2\pi n(\lambda)}$, being λ the wavelength of the wave in vacuum.

As we explain in the previous Section 2.2, energy conservation should be satisfied at the photon level for any nonlinear interaction in a crystal. This is extensible to the momentum conservation

as well, which should be conserver at anytime. For example in the case of the OPO, as there are three different frequencies ω_p, ω_s and ω_i, each wave will have different momentum k: k_p, k_s and k_i. Thus, in the momentum conservation case, the relation between the three waves in an OPO will be expressed as:

$$\Delta k = k_p - k_s - k_i \tag{2.4}$$

If (2.4) results $\Delta k \neq 0$, the phase-mismatch between the three interacting waves in the oscillator, which implies that no specific process is preferred in the cavity and several low-efficiency competing processes would occur simultaneously. However, when the phase-matching is perfect, $\Delta k = 0$, only one nonlinear process of interest is considered. This expression is called phase-matching condition:

$$\Delta k = 0 \tag{2.5}$$

As a result, we can neglect all other nonlinear processes that are possible under the general nonlinear polarization vector expression (2.1) showed in Section 2.1 because they are extremely weak. The phase-matching condition (2.5) applies to processes such as the OPO, SHG and DFG, all in which the tensor χ^2 plays the main role. All these processes are examples of three-wave mixing interactions.

There are two commonly use methods to provide phase-matching. The traditional one works in birefringent crystals compensating for the dispersion by choosing the appropriate polarization of the interacting waves. The second technique is the quasiphase-matching based on periodically poled nonlinear crystals. In the context of this master thesis, we have provided phase matching by birefringent phase-matching.

2.3.1. Birefringent Phase-Matching

Birefringent phase matching is a technique for achieving phase matching of a nonlinear process by exploiting the birefringence of a nonlinear crystal. As birefringent crystals have different indices of refraction at the same wavelength, phase-matching is achieved by the proper choice of wavelengths, polarizations and angles with respect to the crystal's principal axes.

There are two kinds of nonlinear crystals: uniaxial and biaxial crystals, depending upon the number of the axis of anisotropy. Besides, there are two types of BPM for second-order nonlinear processes. Type I and type II. For type I, both signal and idler waves at frequencies have the same polarization and the pump wave is polarized orthogonal compared to the first two. For type II the signal and idler are orthogonally polarized. All electromagnetic waves, polarized transversally to the optical axis and propagating along the optical axis, will sense the same index of refraction.

In the case of the uniaxial crystals, there are two different refractive indexes: the ordinary index of refraction, n_o, and extra-ordinary index of refraction, n_e. The electric field polarized perpendicular to the optical axis will always sense the ordinary index of refraction and this one is called the ordinary beam. The beam polarized orthogonally to the ordinary beam, called the extraordinary beam, has a non-zero projection on the optical axis and senses the extraordinary refractive index, $n_e(\theta)$, which depends on the propagation angle according to the relation:

$$n_e(\theta) = \left[\frac{\sin^2\theta}{n_e^2} + \frac{\cos^2\theta}{n_o^2}\right]^{-1/2} \tag{2.6}$$

where θ is the angle between the optical axis and the propagation direction.

The capability to modify one of the refractive indexes by rotating the crystal this angle θ makes possible to modify the beam trajectory inside of the crystal so, according with the expression (2.6), it makes possible to modify the k vector in order to accomplish the phase-matching condition: $\Delta k = 0$.

The case of biaxial crystals, where $n_x \neq n_y \neq n_z$ are somewhat more complicated and they have been studied thoroughly by Hobden [4].

3. Objective of the experiment

3.1. Frequency combs. Introduction and generation

3.1.1. Introduction to frequency combs

Properties of femtosecond mode-locked lasers open a broad family of potential applications lie in areas such as communications, high speed electronics and signal processing [5]. Thus, they can be used as a 'ruler' to measure frequency intervals as well as it can be used as a 'frequency bridge' to connect distant frequency domains [6], [7]. For this reason, the ability to generate and manipulate very short pulses is highly desirable.

Researchers all over the world have been devoted since 2000 in the development of novel techniques in the family of the frequency combs. Since then, many advantages have been accomplished, until the international recognition in 2005 to Theodor W. Hänsch and John L. Hall. They shared half of the 2005 Nobel Prize in physics for their strong contributions to the development of laser-based precision-spectroscopy, including the optical frequency comb technique. In 2006, new techniques in the femtosecond combs spanned to the extreme ultraviolet regime, enabling frequency metrology in that region of the spectrum apart from the other previously enabled. It might open the door to unprecedented spectral resolution, making it possible for scientists to study the fine structure of atoms and molecules with coherent XUV light [8].

Frequency combs are a very precise tool for measuring different wavelengths —or frequencies— of electromagnetic waves. By recent advances in ultrafast lasers, they can accurately measure much higher frequencies than any other tool. Thus, today they already play an important role in metrology laboratories and physics research and they are starting to become commercially available [1].

In terms of appearance, a frequency comb is a light source which spectrum consists of a series of discrete, equally spaced elements. The strictly knowledge of the space between consecutive elements make possible such a great family of applications. In the frequency domain, it is possible to represent a perfect frequency comb, called Dirac comb, as a series of Dirac´s delta functions spaced according to the expression (see Fig. 3):

$$f(n) = f_0 + n\, f_r \tag{3.1}$$

where n is an integer, f_r is the comb tooth spacing and f_0 is the carrier offset frequency, which is smaller than f_r. This can be used like a ruler to measure the light emitted by lasers, atoms, stars, or other objects with extraordinarily high precision.

Either f_r and f_0 are two degrees of freedom for any frequency comb. As explained above, they can be generated by a broad number of mechanisms, and in any of those the two degrees of freedom can be modulated and stabilized in order to generate a useful comb for mapping optical frequencies into the radio frequency for the direct measurement of optical frequency. The type of laser used to make the comb is critical to the precision of the ruler. The shorter the laser pulses, the broader the range of frequencies in the comb.

The timing between pulses determines the teeth spacing of the frequency comb. Therefore, the faster the pulse repetition rate, the wider the teeth spacing, making each individual tooth easier to identify.

Besides, the stability of the laser determines the width of the individual comb teeth. A highly stabilized laser produces very fine teeth, enabling highly precise measurements of specific frequencies or changes in frequency. Other optical components such as mirrors, special crystals and other techniques also are used to make the comb teeth as perfectly spaced as possible.

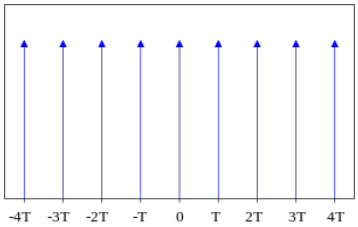

Figure 3. A Dirac comb is an infinite series of Dirac delta functions spaced at intervals of *T* which corresponds with the value of the repetition rate of the pump laser.

3.1.2. Frequency comb´s generation

Amplitude modulation of a continuous wave laser and the stabilization of the pulse train generated by a mode locked laser are the most commonly used methods of frequency comb´s generation. In the context of this master thesis, generation by stabilization of a mode-locked laser is very suitable for our experience. Deep studies about frequency comb´s generation by amplitude modulation of a CW laser were made by K.P. Ho and J.M. Kahn [9].

Mode-locked lasers produce a series of optical pulses separated in time by the round-trip time of the laser cavity. Every single pulse is repeatedly reflected within a mirrored cavity. The pulse has a continuous train of very brief and closely spaced frequencies, regularly spaced in time. In other words,

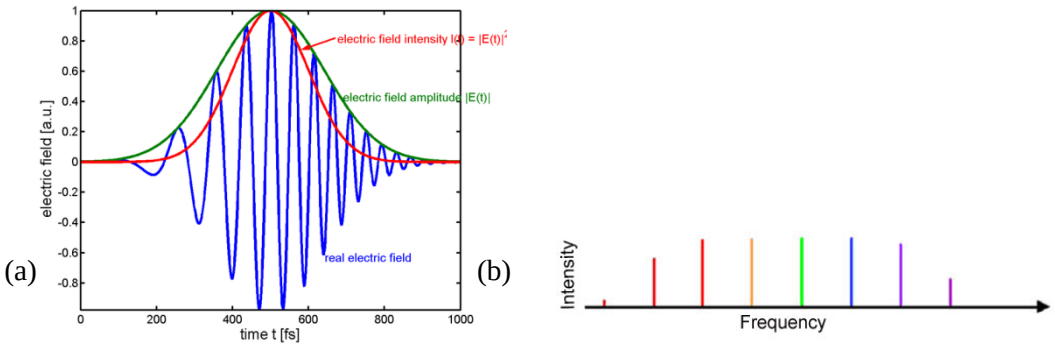

Figure 4. (a) each pulse contains many different frequencies modulated likeness of an envelope. Represented in the time domain; (b) the same electromagnetic waves are represented in the frequency domain. Each "tooth" of the comb is a different color, arranged according to how fast the light wave oscillates in time. It is clear to see that the last one looks like a comb.

3.2. Previous work

In the context of this master thesis, we developed the experiment as the combination of two previous scientific articles in the field of second-order nonlinear conversion by using optical parametric oscillators carried out by A. Esteban-Martin *et al.* at Institute of Photonic Sciences (Spain) and Samuel T. Wong *et al.* at Stanford University (USA).

Femtosecond OPO pumped by a KLM Ti:sapphire laser based on BiB_3O_6 (BIBO) generates signal and idler pulses across 1.4-1.6 μm and 1.6-1.87 μm respectively for collinear type I phase matching in the *xz* optical plane. The high nonlinear gain and large spectral acceptance for type I interaction in the *xz* plane of BIBO permit rapid and continuous tuning across the near infrared range by simple fine adjustment of OPO cavity delay or through small changes in the pump wavelength (in the vicinity of 800 nm). The first demonstration of this effect was reported in [10], providing the rapid, broadband and static tuning features of BIBO crystals in femtosecond OPOs directly pumped by the Ti:sapphire laser.

In addition, the spectral acceptance bandwidth supported by the system becomes very large since the group velocity mismatch (GVM) between signal and idler pulses is very small and vanishes near degeneracy [11]. In particular, is reported that the pump-signal and the pump-idler GVM is less than 1.2 fs/mm and it varies from 35 fs/mm to nearly zero close to degeneracy.

In the other hand, [12] demonstrated a stable degenerate synchronously pumped femtosecond OPO (SPOPO) as a divide-by-2 subharmonic generator by employing a type I phase-matched $MgO:LiNbO_3$ crystal as the nonlinear crystal at 80 MHz mode-locked Ti:sapphire laser with 180 fs pulses pumped at 775 nm. The SPOPO generated transform-limited 70 fs phase-locked output pulses centered at 1550 nm. In the past, implementations of type I degenerate mode-locked OPOs were avoided.

To test the phase-locking between the pump and signal/idler pulses in the degenerate and non degenerate regime, the pump was divided-by-2. The SPOPO signal and idler output (1.5 μm and 1.6 μm aprox. respectively) were frequency doubled (SHG) and after was overlapped with the pump comb at low angle between the beams. The observation of stationary fringes from the interference established phase coherence.

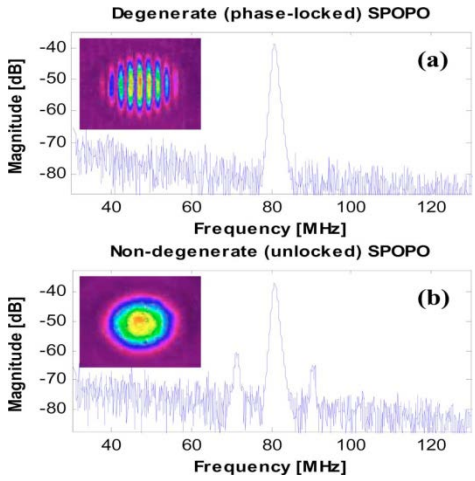

Figure 5. Measurements obtained from frequency doubling the SPOPO output and interfering with the pump: (a) observed fringes and lack of satellite beat notes when phase locked; (b) observed satellite beat notes and lack of fringes when unlocked.

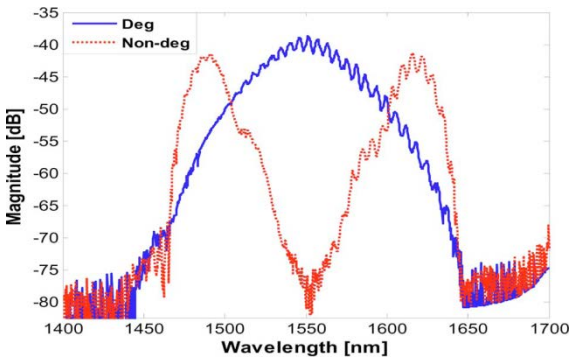

Figure 6. Signal and idler SPOPO spectra for degenerate (blue) and non degenerate regime (red). The degenerate SPOPO forms a broad spectrum centered at 1550 nm. In the non degenerate SPOPO, the signal and idler pulses oscillate at different frequencies.

The SPOPO signal and idler frequencies are half that of the pump and was demonstrated they remain in the phase-locked (degenerate) regime until doubling the SPOPO comb to compare with the pump comb for confirming the phase coherence. It is shown in the Fig. 6 the spectrum of both degenerate and non degenerate signal and idler pulses of the SPOPO.

4. Experimental setup

The configuration of the experimental setup is shown in Fig. 7. The pump laser provides transform-limited pulses at 76 MHz, tunable around 800 nm. At the beginning, a half-wave plate provides extraordinary pump polarization to help the second-order nonlinear processes inside the crystals. The pump is split into two beams: the SPOPO comb and the pump comb. In the SPOPO comb two second-order nonlinear processes are achieved: first OPO in the first crystal and after SHG in the other one.

The SPOPO branch uses two 1.5 mm long BIBO crystals cut for collinear type I ($e \rightarrow o + o$) PM in the *xz* optical plane at an internal angle $\theta = 11.4^{o}$ ($\phi = 0^{o}$) at normal incidence. The end faces have broadband antireflection (AR) coating ($R < 1\%$) for the pump over 800–840nm and for a signal and idler over 1400–1600 nm. A set of lenses, AR coated ($R < 1\%$) at 800nm, are used to focus the beams to a beam waist radius $\omega_0 \approx 25$ μm inside the BIBO crystals and collimate it after to the next step.

The OPO is configured in a standing-wave cavity comprising two concave reflectors M1 and M2 ($r = 100$ mm), one high reflector (HR) plane folding mirror and one plane mirror acting as a 5% output coupler (OC), mounted on a translation stage to allow variation of the cavity length with micrometer precision. The mirrors HR, M1, and M2 are highly reflecting ($R > 99\%$) over 1.45–1.65 μm and highly transmitting ($T > 90\%$) at 800 nm.

The second harmonic generator is configured by a lens which comprises the beam into the BIBO crystal to generate SHG ($o + o \rightarrow e$). A second lens is used to collimate the beam to the beam splitter beyond. A set of spectral filters may be used centered away from the degeneracy to 1.5 or 1.6 μm to block most of the SFG and transmit only the SHG of the signal and the idler.

In order to probe the phase-locking between the pump and signal/idler pulses, the SPOPO signal and idler output were frequency doubled (SHG) by a BIBO crystal and was overlapped beyond –by using a beam splitter– with the pump comb in such a way they set a Mach-Zehnder interferometer. A set of lenses comprised the beam into the crystal and after collimated it again well featured ready to the interferometry in the beam splitter.

The pump comb cavity length was controlled by a delay line mounted on a translation stage to allow the adjustments of the cavity length with micrometer precision.

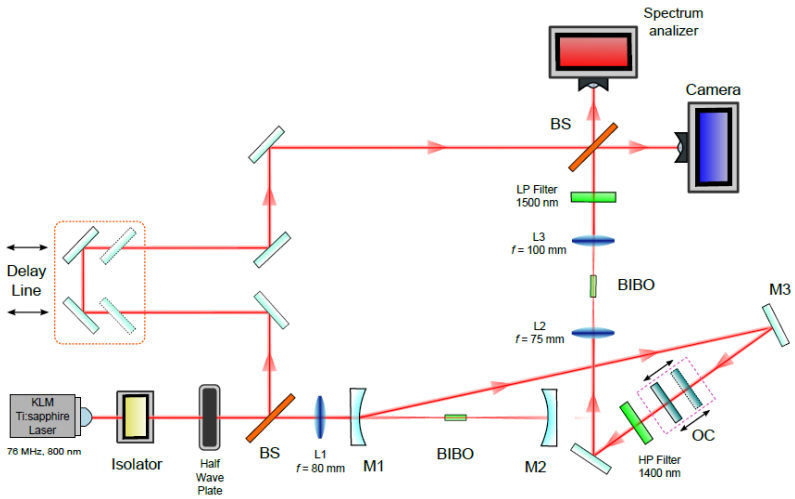

Figure 7. Schematic of the Ti:sapphire-pumped SPOPO as a divided-by-2 subharmonic generator based on the *xz*-cut BIBO with type I ($e \rightarrow o + o$) interaction. The original polarization of the beam from the Ti:sapphire laser is ordinary (perpendicular to the optic table). The HWP changes the polarization of the pump to extraordinary (parallel to the optics table).

5. Results

The experimental results consist in a series of spectrums and images obtained through the high sensibility IR camera and a spectrum analyzer (in blue and in red respectively) (see Fig. 7).

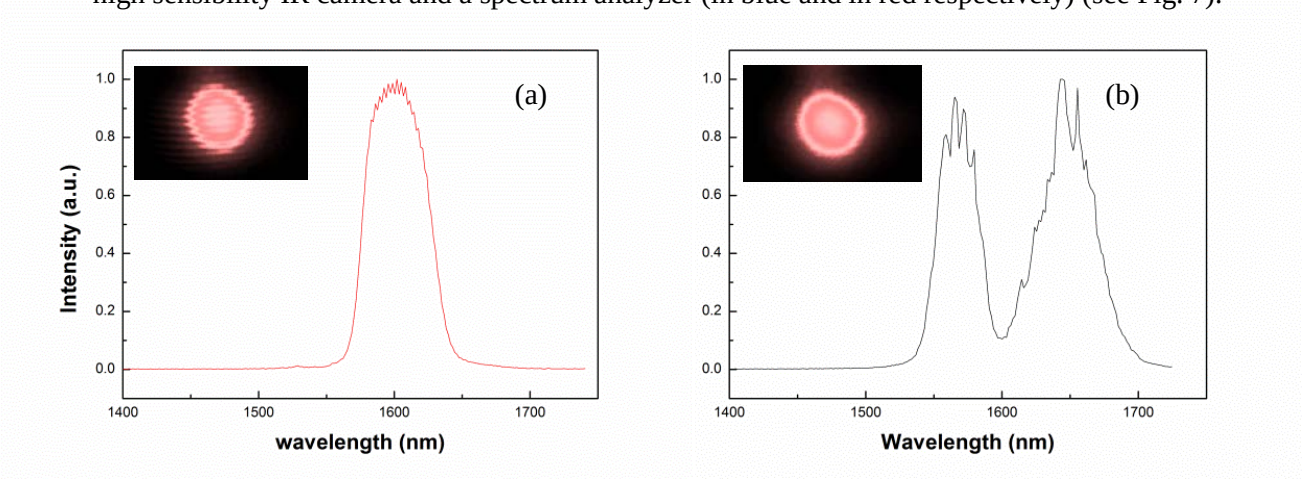

Figure 8. Measurements obtained from frequency doubling de SPOPO output and interfering with the pump for a: (a) degenerated SPOPO and; (b) non degenerated SPOPO.

The reported fringes in Fig. 8 (a) demonstrate the coherence in the degenerated regime of a SPOPO based on BIBO a crystal with type I ($e \rightarrow o + o$) interaction in the *xz* plane. It is worthy to highlight the toothed shape in the top of the spectrum which can suggest the generation of a frequency comb. In the same way, no interference effect is reported in the non degenerated regime (see Fig. 8 (b)).

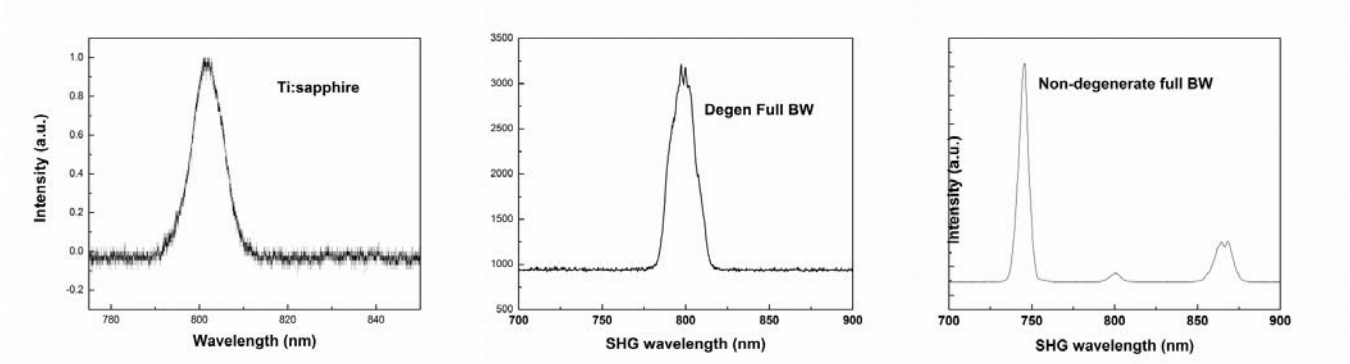

Figure 9. (a) Spectrum of the pump beam; (b) spectrum of the degenerate signal and idler beams after frequency doubling through SHG by a BIBO crystal in the SPOPO comb and; (c) spectrum of the non degenerate signal and idler beams after frequency doubling through SHG by a BIBO crystal in the SPOPO comb.

6. Conclusions

The reported fringes in Fig. 8 (a) demonstrate the coherence in the degenerated regime of a SPOPO based on BIBO a crystal. In the same way, no interference effect is reported in the non degenerated regime (see Fig. 8 (b)). It is worthy to highlight the toothed shape in the top of the spectrum (see Fig. 8 (a)) which can suggest the fact that an optical comb might have been generated. However, it is still under study if this implies a frequency comb generation itself. This is still under research.

In conclusion, we have demonstrated the stability of a degenerated Ti:sapphire pumped femptosecond OPO based on BIBO crystal with type I ($e \rightarrow o + o$) interaction in the *xz* plane. To our knowledge, this is the first demonstration of a self-phase-locked divide-by-2 type I

SPOPO in the *xz* plane of BIBO crystals operating in degenerate regime. The features provided by the resonator as well as the interferometer focused in the development of a more robust and stable frequency comb are currently limited only by the available mirrors and it might be readily extended using more suitable coatings.

It would be suitable to use a set of spectral filters to block 1.5 μm or 1.6 μm frequencies centered away of the degeneracy to block most of the SFG –which always is produced in a BIBO crystal under the conditions reported– and transmit only the SHG of the signal and the idler.

7. Acknowledgements

I acknowledge partial support from the Spanish Ministry of Science and Innovation through the Consolider Program (grant CSD2007-00013) and the European Union (EU) 7th Framework program Mid-Infrared Solid-State Laser Systems for Minimally Invasive Surgery (grant 224042). Also, I acknowledge to Dr. Adolfo Esteban-Martín, Prof. Majid Ebrahim and my other colleges of the group for their unconditional help during the realization of this master thesis.

8. References

[1] US. Dept. of Comerce - The National Institute of Standards and Technology (NIST), «http://www.nist.gov» March 2006.

[2] O. Kokabee, *Chapter II: Theory of Optical Parametric Oscillators*. PhD thesis report: Full design, construction and development of Lasers and Optical Parametric Oscillators.

[3] Encyclopedia of Laser Physics and Technology, «http://www.rp-photonics.com/synchronous_pumping.html»

[4] M. Hobden, *Phase-matched second-harmonic generation in biaxial crystals*, Journal of Applied Physics, **38**(11), 4365 (1967).

[5] W. H. Knox, *Ultrafast technology in telecommunications*, IEEE journal on selected topics in quantum electronics, **6**(6), (2000).

[6] Th. Udem, J. Reichert, R. Holzwarth, and T.W. Hansch, *Accurate measurement of large optical frequency differences with a more-locked laser*, Opt. Lett., **24**(13), 991 (1999).

[7] D.J. Jones et al., *Direct link between microwave and optical frequencies with a 300 THz femtosecond laser comb*, Phys. Rev. Lett., **84**, 51025105 (2000).

[8] Jones et al., *Phase-Coherent Frequency Combs in the Vacuum Ultraviolet via High-Harmonic Generation inside a Femtosecond Enhancement Cavity*, Phys. Rev. Lett., **94**, 193201 (2005).

[9] J.M. Kahn, and K.P. Ho, *Optical frequency comb generator using phase modulation in amplified circulating loop*, Phot. Tech. Lett. IEEE, **5**(6), 721 (1993).

[10] A. Esteban-Martin, V. Ramaiah-Badarla, V. Petrov, and M. Ebrahim-Zadeh, *Broadband, rapidly tunable Ti:sapphire-pumped BiB3O6 femtosecond optical parametric oscillator*, Opt. Lett., **36**(9), 1671 (2011).

[11] V. Petrov, F. Noack, P. Tzankov, M. Ghotbi, M. Ebrahim-Zadeh, I. Nikolov, and I. Buchvarov, *Opt. Express,* **15**, 556 (2007).

[12] Samuel T. Wong, Tomas Plettner, Konstantin L. Vodopyanov, Karel Urbanek, Michel Digonnet, and Robert L. Byer, *Self-phase-locked degenerate femtosecond optical parametric oscillator*, Opt. Lett., **33**(16), 1896 (2008).